JACS
JOURNAL OF THE AMERICAN CHEMICAL SOCIETY
pubs.acs.org/JACS
Communication

Supramolecular Reinforcement of a Large-Pore 2D Covalent Organic Framework

Shashini D. Diwakara, Whitney S. Y. Ong, Yalini H. Wijesundara, Robert L. Gearhart, Fabian C. Herbert, Sarah G. Fisher, Gregory T. McCandless, Sampath B. Alahakoon, Jeremiah J. Gassensmith, Sheel C. Dodani, and Ronald A. Smaldone*

Cite This: https://doi.org/10.1021/jacs.1c12020
Read Online

ABSTRACT: Two-dimensional covalent organic frameworks (2D-COFs) are a class of crystalline porous organic polymers that consist of covalently linked, two-dimensional sheets that can stack together through noncovalent interactions. Here we report the synthesis of a novel COF, called PyCOFamide, which has an experimentally observed pore size that is greater than 6 nm in diameter. This is among the largest pore size reported to date for a 2D-COF. PyCOFamide exhibits permanent porosity and high crystallinity as evidenced by the nitrogen adsorption, powder X-ray diffraction, and high-resolution transmission electron microscopy. We show that the pore size of PyCOFamide is large enough to accommodate fluorescent proteins such as Superfolder green fluorescent protein and mNeonGreen. This work demonstrates the utility of noncovalent structural reinforcement in 2D-COFs to produce larger and persistent pore sizes than previously possible.

Two-dimensional covalent organic frameworks (2D-COFs) are crystalline, porous, organic polymer networks built from organic monomers and linked together by dynamic covalent bonds.[1−3] Researchers have explored the landscape of COF structures for use in applications such as molecular separation,[4,5] sensing,[6,7] gas storage,[8,9] electronic devices,[10,11] and catalysis.[12,13] COFs can be designed for various applications by modifying their crystallinity, pore size, and surface area from the bottom up.[3,14−16]

One fundamental challenge in porous materials design involves the synthesis of structures with large and persistent pores. There are several obstacles in this pursuit, including the solubility of large organic molecules needed to generate the large-pore sizes[17,18] as well as the propensity for pore collapse or structural damage upon solvent removal.[19−23] As a result, 2D-COFs with a pore diameter larger than 5 nm are not common (Table S1).[14,24−26] There are additional challenges in the design of large-pore 2D-COFs as they use more flexible organic linkages[27−30] in the covalent sheets compared with more rigid metal−organic frameworks (MOFs)[17] along with the potential for inefficient stacking of the layers in an eclipsed orientation.[31,32] These 2D sheets are held together by noncovalent interactions such as donor−acceptor complexes,[15] aromatic stacking interactions,[15,33,34] dipole−dipole interactions,[35,36] van der Waals forces,[37] and hydrogen bonding.[38−43] A number of methods to improve the crystallinity and surface area of 2D-COFs have been extensively studied.[15,33,44,45] COF activation methods have evolved to include the use of fluorous liquids[27] or supercritical carbon dioxide ($scCO_2$)[28−30] to remove organic solvents used during the polymerization. This strategy is beneficial as it can be used on any material and does not require any synthetic modification of the COF structure. However, more recent work has shown that by designing

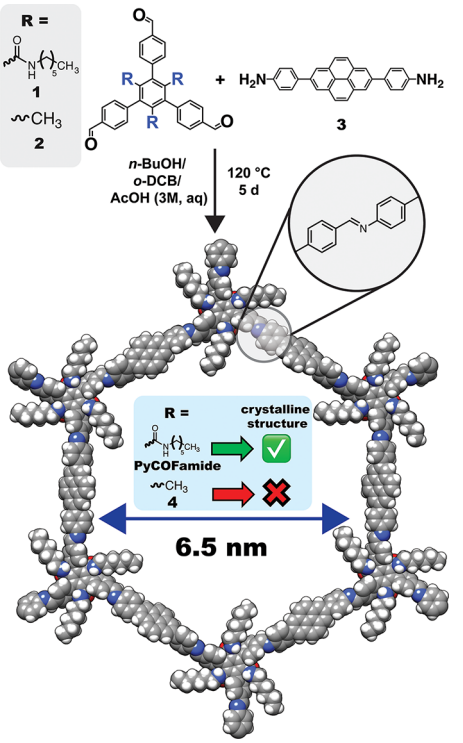

Figure 1. Synthesis and structure of PyCOFamide.

Received: November 15, 2021

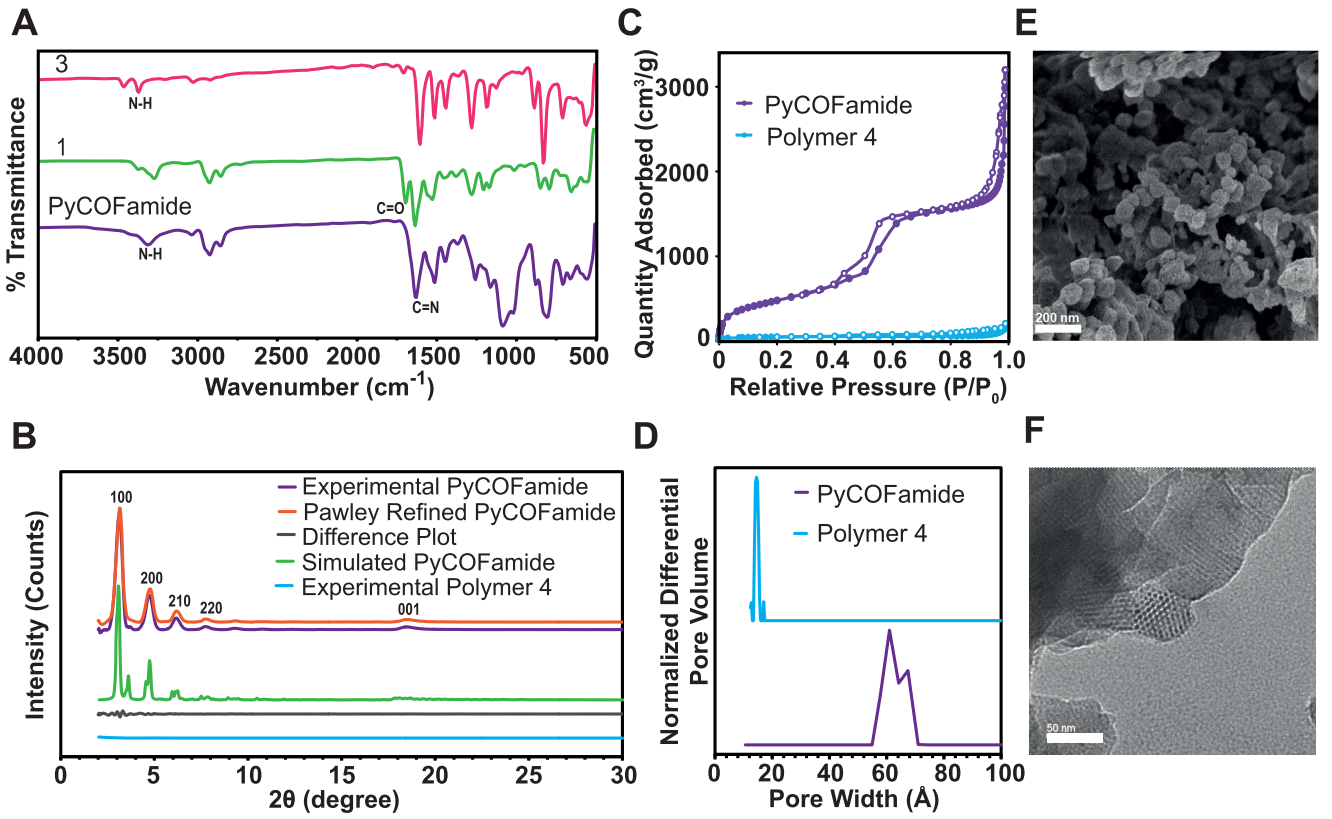

Figure 2. (A) FT-IR spectra of PyCOFamide and starting monomers. (B) PXRD patterns of PyCOFamide (purple), Pawley refined (red), simulated PyCOFamide (green), difference plot (black), and experimental polymer **4** (blue). (C) Nitrogen adsorption (closed circles) and desorption (open circles) isotherm for PyCOFamide (purple) and polymer **4** (blue). (D) Pore size distributions for PyCOFamide and control polymer **4**. (E) SEM of PyCOFamide. (F) HR-TEM of PyCOFamide.

noncovalent interactions that are directed specifically between the layers, COFs with significantly improved crystallinity and surface area can be attained, even without $scCO_2$ activation.[15,26,43,45] However, as pore sizes increase, even the gentlest solvent activation methods can cause damage to the structure. In these situations, the only way to preserve these large pores may be through a combination of structural reinforcement and improved activation methods. Here we present a supramolecular reinforcement strategy that strengthens the adhesion between the stacked 2D COF layers through the use of directed hydrogen bonding and stabilizes the large pores against collapse.

Our group recently reported a class of 2D-COFs with secondary amide side chains that can facilitate interlayer hydrogen bonding (COFamide 1−2).[43] Given our previous observation that the highly correlated interlayer hydrogen bonding of the COFamide series made them resistant to pore collapse using conventional solvent activation conditions, we aimed to expand the pore size with the expectation that the rigidified layer structure could support larger pores. In this study, we polymerized a tritopic aldehyde with amide side chains (**1**) and a ditopic amine linker 4,4′-(pyrene-2,7-diyl)dianiline (**3**) to produce the imine-linked PyCOFamide (Figure 1). A control polymer without amide groups was synthesized (**4**) with methyl groups in place of the secondary amide groups (**2**) to investigate the importance of the interlayer hydrogen bonding on the COF structure. Polymerization reactions were performed in a solvent mixture of *o*-dichlorobenzene, *n*-butanol, and acetic acid (3 M, aq) in a ratio of 1.9:1:0.1 at 120 °C for 5 days to produce PyCOFamide or polymer **4**. The insoluble polymers obtained were activated by using $scCO_2$ before further characterization. The PyCOFamide was obtained as an ash-colored powder whereas **4** was a light-yellow powder. These are insoluble in common organic solvents such as acetone, methanol, dichloromethane, and hexane.

The FT-IR spectrum of PyCOFamide (Figure 2A) showed the appearance of a signal at 1628 cm^{-1}, which is characteristic of an imine stretching vibration. The disappearance of the aldehyde C═O stretching modes at 1697 cm^{-1} and amine N−H vibrations at 3464 cm^{-1} confirms the absence of starting monomers in the final polymer. Additionally, the amide N−H stretching vibrations of PyCOFamide shift to 3309 cm^{-1} compared to the amide N−H stretching modes of **1** at 3278 cm^{-1}. This shift can be attributed to the formation of interlayer hydrogen-bonding interactions.[43] We digested PyCOFamide in acidic DMSO-d_6 to determine the monomer incorporation ratio. We found the aldehyde to amine monomer ratio to be 1:1.5, which is consistent with the initial feed ratio (Figure S11).

Powder X-ray diffraction (PXRD) experiments were performed to determine the crystallinity. Sharp diffraction peaks were observed in the $scCO_2$ activated PyCOFamide. An intense and narrow diffraction peak corresponding to the (100) crystal plane was observed at 3.1° 2θ in the PyCOFamide diffraction pattern (Figure 2B). Other peaks were observed at 4.8°, 6.2°, 7.8°, 9.4°, 10.9°, and 18.5° which can be attributed to the diffraction from the (110), (200), (210), (120), (220), and (001) crystal planes. The experimental and simulated PXRD patterns of PyCOFamide

https://doi.org/10.1021/jacs.1c12020
J. Am. Chem. Soc. XXXX, XXX, XXX−XXX

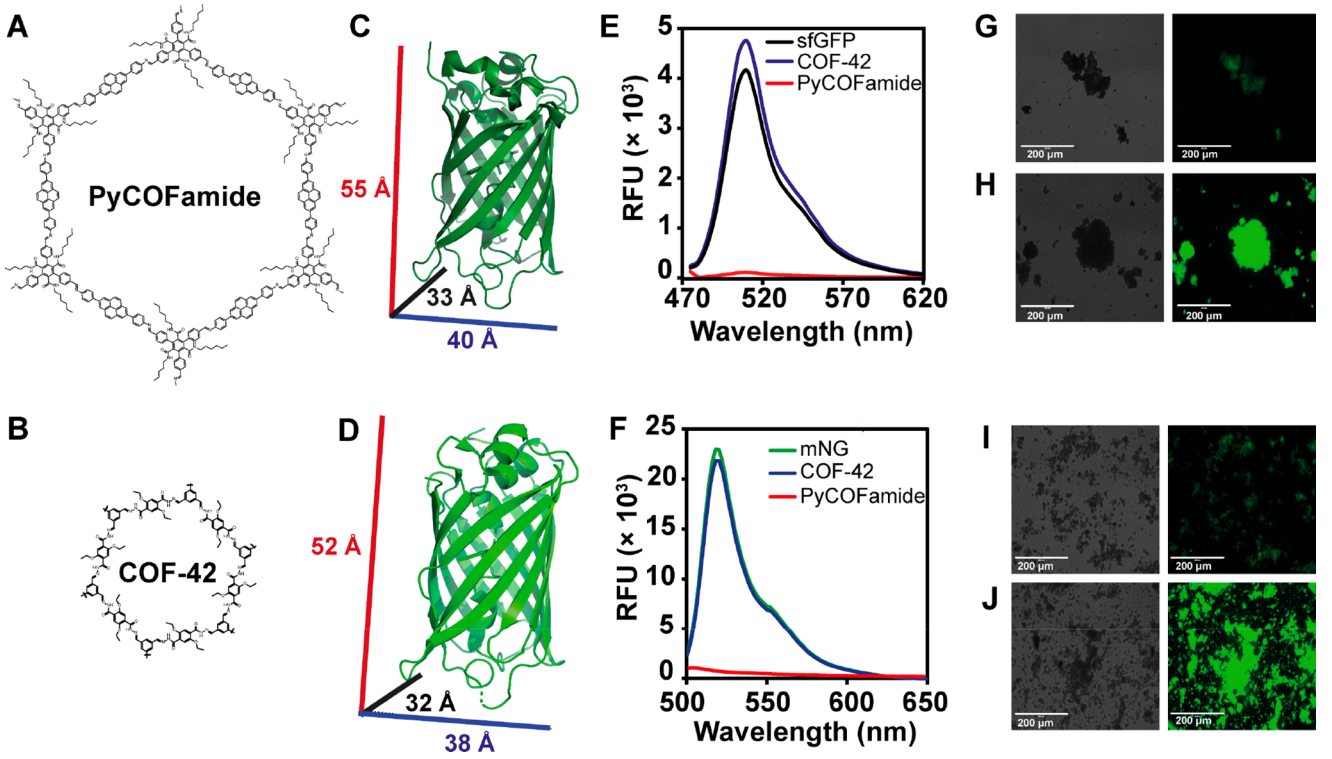

Figure 3. Structure of (A) PyCOFamide and (B) COF-42. Dimensions of (C) sfGFP (PDB ID: 2B3P) and (D) mNG (PDB ID: 5LTR). Fluorescence spectra of (E) sfGFP loading into PyCOFamide and COF-42. (F) mNG loading into PyCOFamide and COF-42. Fluorescence microscopy images of (G) sfGFP loaded COF-42 pellet, (H) sfGFP loaded PyCOFamide pellet, (I) mNG loaded COF-42 pellet, and (J) mNG loaded PyCOFamide pellet.

match well and help confirm the presence of key structural features found in the eclipsed stacking arrangement (Figure S6). The (001) reflection for PyCOFamide appears at 18.5°, which is characteristic for COFamides as they have larger interlayer spacing distances because of the steric hindrance caused by the out-of-plane phenyl rings and amide groups at the node positions.[43] The interlayer distance predicted from the simulated crystal structure (~5.1 Å) is similar to the experimental value (~4.8 Å) obtained from PXRD. No peaks were observed in polymer **4** PXRD pattern (Figure 2B), indicating its amorphous nature due to either pore collapse or poor 2D sheet stacking.

The Brunauer–Emmett–Teller (BET) surface area and pore size distributions of PyCOFamide and **4** were measured by nitrogen adsorption measurements (Figure 2C). $scCO_2$ activated PyCOFamide has a BET surface area of 1682 m^2/g. However, under conventional activation (washing with organic solvents and heating under dynamic vacuum >10 μmHg), the BET surface area is significantly lower (8 m^2/g) (Figure S5). Pore collapse or decrystallization is common in conventional solvent activation because of the capillary effect that occurs during solvent evaporation under vacuum.[30] In comparison, the control polymer **4** has a low accessible surface area (169 m^2/g) and no observable crystallinity regardless of activation method, indicating that the hydrogen-bonding interactions are key to reinforcing the eclipsed stacking mode. PyCOFamide has a type IV isotherm, which is characteristic of mesoporous materials (pores >20 Å). PyCOFamide has a narrow pore size distribution at 61 and 67 Å (Figure 2D) which agrees with the calculated pore size (65 Å) from the computational model with eclipsed stacking (Figure S6).

Scanning electron microscopy (SEM) images of the PyCOFamide powder reveal discotic morphology (Figure 2E) with aggregated discs about 70 nm in size. The highly ordered, periodic structure of PyCOFamide was observed in the high-resolution transmission electron microscope (HR-TEM) image (Figure 2F). This clearly shows the hexagonal pore arrangement indicating long-range order in PyCOFamide. These observations are consistent with the PXRD data. The size of the hexagonal pores is also in agreement with those obtained from the nitrogen adsorption isotherm.

To test the stability of PyCOFamide, the COF was immersed in various aqueous solutions and organic solvents such as *N*,*N*-dimethylformamide (DMF), dimethyl sulfoxide (DMSO), 1,4-dioxane, *N*-methyl-2-pyrrolidone (NMP), sulfuric acid (1 M, aq), sodium hydroxide (1 M, aq), and phosphate buffered saline (PBS, pH = 7.4). The retention of crystallinity after immersion was studied by PXRD (Figure S10). The results revealed that the crystallinity of PyCOFamide is retained in DMF, sodium hydroxide, and PBS. However, the crystallinity of PyCOFamide is damaged in the sulfuric acid, which may be due to hydrolysis of the imine linkages under acidic conditions. Additionally, PyCOFamide crystallinity was lost in 1,4-dioxane, DMSO, and NMP solvents likely due to their polarity that could exfoliate or displace the COF layers. Interestingly, the peak at 18.5°, characteristic of the interlayer stacking distance in COFamide-based materials, remains visible in the PXRD patterns even after the other peaks have disappeared. We hypothesize that this could arise from continued stacking between disordered sheets after decrystallization.

The large pores of PyCOFamide (Figure 3A), combined with its stability in aqueous solutions like PBS, encouraged us

https://doi.org/10.1021/jacs.1c12020
J. Am. Chem. Soc. XXXX, XXX, XXX–XXX

to study its ability to host proteins. Porous materials, including MOFs,[17,46−48] COFs,[49−52] mesoporous silica,[53,54] hydrogen-bonded organic frameworks,[55] zeolites,[56] and cage compounds,[57] have been used to adsorb a variety of biomolecules as guests into their pores. Once inside the pores of a polymer, the reactive properties or stability can be greatly affected. However, the inclusion of biomolecules into the individual pores of COFs is less common because the pore sizes of 2D-COFs are often too small to host an entire protein. As a proof-of concept, we selected two β-barrel fluorescent proteins: Superfolder green fluorescent protein (sfGFP)[58,59] (Figure 3C) and mNeonGreen (mNG)[60] (Figure 3D). The approximate dimensions of selected proteins would allow for encapsulation within PyCOFamide, and the infiltration of protein into the COF pores can be easily monitored by using fluorescence spectroscopy and fluorescence microscopic imaging. COF-42 (Figure 3B),[61] which has a smaller pore diameter (2.3 nm) than $scCO_2$ activated PyCOFamide, was used as a control since both proteins are too big to fit into its pores. Additionally, previous work in MOF-based protein adsorption has shown that hydrophobic side chains, like those found in COF-42 and PyCOFamide, are favorable for the adsorption of GFP.[17] We prepared samples with different COF-to-protein ratios and monitored the fluorescence signal of both sfGFP and mNG in solutions before and after PyCOFamide or COF-42 were added to them. In the ratio of COF to protein at 9:1, we observed that the fluorescence of the supernatant of both proteins drastically decreased when PyCOFamide was added, whereas the solutions containing COF-42 do not (Figure 3E,F), indicating both proteins are being drawn out of solution and into the pores of PyCOFamide.

We further confirmed the inclusion of protein in the pores of PyCOFamide using fluorescence microscopy to directly observe changes in fluorescence of the solid COFs before and after addition of protein. Some fluorescence is observable in COF-42 samples (Figure 3G, Figure S18, Figure 3I, and Figure S21) which is likely attributed to surface adsorption of the proteins on the COF particles through interactions of the proteins with the functional groups at the pore edges or trapping within interparticle voids. In contrast, PyCOFamide particles are highly fluorescent, indicating a greater extent of protein inclusion (Figure 3H,J). Because the mass of COF powder used in each of these experiments is the same, the amount of particle surface should be similar for both COF-42 and PyCOFamide. Therefore, the difference in protein adsorption between these COFs can be attributed to the fact that the large pores of PyCOFamide are accessible to the sfGFP and mNG whereas the small pores of COF-42 are not. The retention of fluorescence for sfGFP and mNG in PyCOFamide indicates that the proteins are not denatured and retain their structure after adsorption within the COF.

In conclusion, we have designed and synthesized a novel large-pore COF whose structure is stabilized through interlayer hydrogen bonding. PyCOFamide exhibits large-pore channels of >6 nm in diameter, which are among the largest reported to date in a 2D-COF. The interlayer hydrogen bonding in PyCOFamide is key to its ability to maintain its structure after activation, as similar monomers incapable of hydrogen bonding do not produce ordered COFs. The design strategies for making large-pore 2D-COFs in the future will necessitate design approaches that consider both mild activation techniques (e.g., $scCO_2$) and the supramolecular interactions between the layers.[3,24,26,36,45] We have also demonstrated that large biomolecules such as fluorescent proteins can be loaded into the pores of PyCOFamide without loss of their function, suggesting that these COFs could potentially be used in the future as hosts for enzymes or biosensing proteins or as delivery vehicles for biomolecule-based therapeutics. Taken together, our study sets the stage for expanding the scope of COF chemistry providing a supramolecular design strategy to synthesize COFs with large persistent pores.

■ ASSOCIATED CONTENT

Supporting Information

The Supporting Information is available free of charge at https://pubs.acs.org/doi/10.1021/jacs.1c12020.

Synthesis procedures of the COFs and additional data including NMR spectra, solvent stability, and protein infiltration (PDF)

■ AUTHOR INFORMATION

Corresponding Author

Ronald A. Smaldone − *Department of Chemistry and Biochemistry, University of Texas at Dallas, Richardson, Texas 75080, United States;* orcid.org/0000-0003-4560-7079; Email: ronald.smaldone@utdallas.edu

Authors

Shashini D. Diwakara − *Department of Chemistry and Biochemistry, University of Texas at Dallas, Richardson, Texas 75080, United States*

Whitney S. Y. Ong − *Department of Chemistry and Biochemistry, University of Texas at Dallas, Richardson, Texas 75080, United States;* orcid.org/0000-0001-9821-9972

Yalini H. Wijesundara − *Department of Chemistry and Biochemistry, University of Texas at Dallas, Richardson, Texas 75080, United States*

Robert L. Gearhart − *Department of Chemistry and Biochemistry, University of Texas at Dallas, Richardson, Texas 75080, United States*

Fabian C. Herbert − *Department of Chemistry and Biochemistry, University of Texas at Dallas, Richardson, Texas 75080, United States*

Sarah G. Fisher − *Department of Chemistry and Biochemistry, University of Texas at Dallas, Richardson, Texas 75080, United States*

Gregory T. McCandless − *Department of Chemistry and Biochemistry, University of Texas at Dallas, Richardson, Texas 75080, United States*

Sampath B. Alahakoon − *Institute of Combinatorial Advanced Research and Education, General Sir John Kotelawala Defence University, Ratmalana 10390, Sri Lanka*

Jeremiah J. Gassensmith − *Department of Chemistry and Biochemistry and Department of Bioengineering, University of Texas at Dallas, Richardson, Texas 75080, United States;* orcid.org/0000-0001-6400-8106

Sheel C. Dodani − *Department of Chemistry and Biochemistry, University of Texas at Dallas, Richardson, Texas 75080, United States;* orcid.org/0000-0003-0271-6080

Complete contact information is available at: https://pubs.acs.org/10.1021/jacs.1c12020

Notes

The authors declare no competing financial interest.

■ ACKNOWLEDGMENTS

R.A.S. acknowledges support from the Army Research Laboratory (W911NF-18-2-0035). S.C.D. acknowledges support from UT Dallas, the Welch Foundation (AT-2060-20210327), and the National Institute of General Medical Sciences of the National Institutes of Health (R35GM128923). J.J.G. acknowledges the Robert A. Welch Foundation (Grant AT-1989-20190330) for funding this research and the NSF (Grants CAREER Award DMR-1654405 and DMR-2003534) for funding the integration of his entire scholarly and educational activities. This work is the sole responsibility of the authors and does not represent the views of the funding sources.

■ REFERENCES

(1) Côté, A. P.; Benin, A. I.; Ockwig, N. W.; O'Keeffe, M.; Matzger, A. J.; Yaghi, O. M. Porous, Crystalline, Covalent Organic Frameworks. *Science* **2005**, *310*, 1166−1170.

(2) Geng, K.; He, T.; Liu, R.; Dalapati, S.; Tan, K. T.; Li, Z.; Tao, S.; Gong, Y.; Jiang, Q.; Jiang, D. Covalent Organic Frameworks: Design, Synthesis, and Functions. *Chem. Rev.* **2020**, *120*, 8814−8933.

(3) Alahakoon, S. B.; Diwakara, S. D.; Thompson, C. M.; Smaldone, R. A. Supramolecular Design in 2D Covalent Organic Frameworks. *Chem. Soc. Rev.* **2020**, *49*, 1344−1356.

(4) Lohse, M. S.; Stassin, T.; Naudin, G.; Wuttke, S.; Ameloot, R.; de Vos, D.; Medina, D. D.; Bein, T. Sequential Pore Wall Modification in a Covalent Organic Framework for Application in Lactic Acid Adsorption. *Chem. Mater.* **2016**, *28*, 626−631.

(5) Kandambeth, S.; Biswal, B. P.; Chaudhari, H. D.; Rout, K. C.; Kunjattu, H. S.; Mitra, S.; Karak, S.; Das, A.; Mukherjee, R.; Kharul, U. K.; Banerjee, R. Selective Molecular Sieving in Self-Standing Porous Covalent-Organic-Framework Membranes. *Adv. Mater.* **2017**, *29*, 1603945.

(6) Ascherl, L.; Evans, E. W.; Hennemann, M.; di Nuzzo, D.; Hufnagel, A. G.; Beetz, M.; Friend, R. H.; Clark, T.; Bein, T.; Auras, F. Solvatochromic Covalent Organic Frameworks. *Nat. Commun.* **2018**, *9*, 3802.

(7) Jhulki, S.; Evans, A. M.; Hao, X.-L.; Cooper, M. W.; Feriante, C. H.; Leisen, J.; Li, H.; Lam, D.; Hersam, M. C.; Barlow, S.; Brédas, J.-L.; Dichtel, W. R.; Marder, S. R. Humidity Sensing through Reversible Isomerization of a Covalent Organic Framework. *J. Am. Chem. Soc.* **2020**, *142*, 783−791.

(8) Furukawa, H.; Yaghi, O. M. Storage of Hydrogen, Methane, and Carbon Dioxide in Highly Porous Covalent Organic Frameworks for Clean Energy Applications. *J. Am. Chem. Soc.* **2009**, *131*, 8875−8883.

(9) Ma, H.; Ren, H.; Meng, S.; Yan, Z.; Zhao, H.; Sun, F.; Zhu, G. A 3D Microporous Covalent Organic Framework with Exceedingly High C_3H_8/CH_4 and C_2 Hydrocarbon/CH_4 Selectivity. *Chem. Commun.* **2013**, *49*, 9773−9775.

(10) Samanta, P.; Desai, A. v.; Anothumakkool, B.; Shirolkar, M. M.; Karmakar, A.; Kurungot, S.; Ghosh, S. K. Enhanced Proton Conduction by Post-Synthetic Covalent Modification in a Porous Covalent Framework. *J. Mater. Chem.* **2017**, *5*, 13659−13664.

(11) Wang, M.; Wang, M.; Lin, H.-H.; Ballabio, M.; Zhong, H.; Bonn, M.; Zhou, S.; Heine, T.; Cánovas, E.; Dong, R.; Feng, X. High-Mobility Semiconducting Two-Dimensional Conjugated Covalent Organic Frameworks with p-Type Doping. *J. Am. Chem. Soc.* **2020**, *142*, 21622−21627.

(12) Xu, H.; Chen, X.; Gao, J.; Lin, J.; Addicoat, M.; Irle, S.; Jiang, D. Catalytic Covalent Organic Frameworks via Pore Surface Engineering. *Chem. Commun.* **2014**, *50*, 1292−1294.

(13) Lin, S.; Diercks, C. S.; Zhang, Y.-B.; Kornienko, N.; Nichols, E. M.; Zhao, Y.; Paris, A. R.; Kim, D.; Yang, P.; Yaghi, O. M.; Chang, C. J. Covalent Organic Frameworks Comprising Cobalt Porphyrins for Catalytic CO_2 Reduction in Water. *Science* **2015**, *349*, 1208−1213.

(14) Li, Z.; He, T.; Gong, Y.; Jiang, D. Covalent Organic Frameworks: Pore Design and Interface Engineering. *Acc. Chem. Res.* **2020**, *53*, 1672−1685.

(15) Chen, X.; Addicoat, M.; Irle, S.; Nagai, A.; Jiang, D. Control of Crystallinity and Porosity of Covalent Organic Frameworks by Managing Interlayer Interactions Based on Self-Complementary π-Electronic Force. *J. Am. Chem. Soc.* **2013**, *135*, 546−549.

(16) Huang, N.; Wang, P.; Jiang, D. Covalent Organic Frameworks: A Materials Platform for Structural and Functional Designs. *Nat. Rev. Mater.* **2016**, *1*, 16068.

(17) Deng, H.; Grunder, S.; Cordova, K. E.; Valente, C.; Furukawa, H.; Hmadeh, M.; Gandara, F.; Whalley, A. C.; Liu, Z.; Asahina, S.; Kazumori, H.; O'Keeffe, M.; Terasaki, O.; Stoddart, J. F.; Yaghi, O. M. Large-Pore Apertures in a Series of Metal-Organic Frameworks. *Science* **2012**, *336*, 1018−1023.

(18) Chen, B.; Eddaoudi, M.; Hyde, S. T.; O'Keeffe, M.; Yaghi, O. M. Interwoven Metal-Organic Framework on a Periodic Minimal Surface with Extra-Large Pores. *Science* **2001**, *291*, 1021−1023.

(19) Farha, O. K.; Hupp, J. T. Rational Design, Synthesis, Purification, and Activation of Metal−Organic Framework Materials. *Acc. Chem. Res.* **2010**, *43*, 1166−1175.

(20) Nelson, A. P.; Farha, O. K.; Mulfort, K. L.; Hupp, J. T. Supercritical Processing as a Route to High Internal Surface Areas and Permanent Microporosity in Metal−Organic Framework Materials. *J. Am. Chem. Soc.* **2009**, *131*, 458−460.

(21) Mondloch, J. E.; Karagiaridi, O.; Farha, O. K.; Hupp, J. T. Activation of Metal−Organic Framework Materials. *CrystEngComm* **2013**, *15*, 9258−9264.

(22) Liu, B.; Wong-Foy, A. G.; Matzger, A. J. Rapid and Enhanced Activation of Microporous Coordination Polymers by Flowing Supercritical CO_2. *Chem. Commun.* **2013**, *49*, 1419−1421.

(23) Furukawa, H.; Gándara, F.; Zhang, Y.-B.; Jiang, J.; Queen, W. L.; Hudson, M. R.; Yaghi, O. M. Water Adsorption in Porous Metal−Organic Frameworks and Related Materials. *J. Am. Chem. Soc.* **2014**, *136*, 4369−4381.

(24) Jin, S.; Furukawa, K.; Addicoat, M.; Chen, L.; Takahashi, S.; Irle, S.; Nakamura, T.; Jiang, D. Large Pore Donor−Acceptor Covalent Organic Frameworks. *Chem. Sci.* **2013**, *4*, 4505−4511.

(25) Zhao, C.; Lyu, H.; Ji, Z.; Zhu, C.; Yaghi, O. M. Ester-Linked Crystalline Covalent Organic Frameworks. *J. Am. Chem. Soc.* **2020**, *142*, 14450−14454.

(26) Emmerling, S. T.; Schuldt, R.; Bette, S.; Yao, L.; Dinnebier, R. E.; Kästner, J.; Lotsch, B. V. Interlayer Interactions as Design Tool for Large-Pore COFs. *J. Am. Chem. Soc.* **2021**, *143*, 15711−15722.

(27) Zhu, D.; Verduzco, R. Ultralow Surface Tension Solvents Enable Facile COF Activation with Reduced Pore Collapse. *ACS Appl. Mater. Interfaces* **2020**, *12*, 33121−33127.

(28) Diwakara, S. D.; McCandless, G. T.; Alahakoon, S. B.; Smaldone, R. A. Synthesis of Side-Chain-Free Hydrazone-Linked Covalent Organic Frameworks through Supercritical Carbon Dioxide Activation. *Organic Materials* **2021**, *03*, 277−282.

(29) Sick, T.; Rotter, J. M.; Reuter, S.; Kandambeth, S.; Bach, N. N.; Döblinger, M.; Merz, J.; Clark, T.; Marder, T. B.; Bein, T.; Medina, D. D. Switching on and off Interlayer Correlations and Porosity in 2D Covalent Organic Frameworks. *J. Am. Chem. Soc.* **2019**, *141*, 12570−12581.

(30) Feriante, C. H.; Jhulki, S.; Evans, A. M.; Dasari, R. R.; Slicker, K.; Dichtel, W. R.; Marder, S. R. Rapid Synthesis of High Surface Area Imine-Linked 2D Covalent Organic Frameworks by Avoiding Pore Collapse During Isolation. *Adv. Mater.* **2020**, *32*, 1905776.

(31) Alahakoon, S. B.; Thompson, C. M.; Nguyen, A. X.; Occhialini, G.; McCandless, G. T.; Smaldone, R. A. An Azine-Linked Hexaphenylbenzene Based Covalent Organic Framework. *Chem. Commun.* **2016**, *52*, 2843−2845.

(32) Thompson, C. M.; Occhialini, G.; McCandless, G. T.; Alahakoon, S. B.; Cameron, V.; Nielsen, S. O.; Smaldone, R. A. Computational and Experimental Studies on the Effects of Monomer

https://doi.org/10.1021/jacs.1c12020
J. Am. Chem. Soc. XXXX, XXX, XXX−XXX

Planarity on Covalent Organic Framework Formation. *J. Am. Chem. Soc.* **2017**, *139*, 10506−10513.
(33) Alahakoon, S. B.; McCandless, G. T.; Karunathilake, A. A. K.; Thompson, C. M.; Smaldone, R. A. Enhanced Structural Organization in Covalent Organic Frameworks Through Fluorination. *Chem.—Eur. J.* **2017**, *23*, 4255−4259.
(34) Alahakoon, S. B.; Occhialini, G.; McCandless, G. T.; Karunathilake, A. A. K.; Nielsen, S. O.; Smaldone, R. A. Experimental and Theoretical Insight into the Effect of Fluorine Substituents on the Properties of Azine Linked Covalent Organic Frameworks. *CrystEngComm* **2017**, *19*, 4882−4885.
(35) Salonen, L. M.; Medina, D. D.; Carbó-Argibay, E.; Goesten, M. G.; Mafra, L.; Guldris, N.; Rotter, J. M.; Stroppa, D. G.; Rodríguez-Abreu, C. A Supramolecular Strategy Based on Molecular Dipole Moments for High-Quality Covalent Organic Frameworks. *Chem. Commun.* **2016**, *52*, 7986−7989.
(36) Spitler, E. L.; Koo, B. T.; Novotney, J. L.; Colson, J. W.; Uribe-Romo, F. J.; Gutierrez, G. D.; Clancy, P.; Dichtel, W. R. A 2D Covalent Organic Framework with 4.7-nm Pores and Insight into Its Interlayer Stacking. *J. Am. Chem. Soc.* **2011**, *133*, 19416−19421.
(37) Smith, B. J.; Hwang, N.; Chavez, A. D.; Novotney, J. L.; Dichtel, W. R. Growth Rates and Water Stability of 2D Boronate Ester Covalent Organic Frameworks. *Chem. Commun.* **2015**, *51*, 7532−7535.
(38) Halder, A.; Karak, S.; Addicoat, M.; Bera, S.; Chakraborty, A.; Kunjattu, S. H.; Pachfule, P.; Heine, T.; Banerjee, R. Ultrastable Imine-Based Covalent Organic Frameworks for Sulfuric Acid Recovery: An Effect of Interlayer Hydrogen Bonding. *Angew. Chem., Int. Ed.* **2018**, *57*, 5797−5802.
(39) Halder, A.; Ghosh, M.; Khayum M, A.; Bera, S.; Addicoat, M.; Sasmal, H. S.; Karak, S.; Kurungot, S.; Banerjee, R. Interlayer Hydrogen-Bonded Covalent Organic Frameworks as High-Performance Supercapacitors. *J. Am. Chem. Soc.* **2018**, *140*, 10941−10945.
(40) Zhao, C.; Diercks, C. S.; Zhu, C.; Hanikel, N.; Pei, X.; Yaghi, O. M. Urea-Linked Covalent Organic Frameworks. *J. Am. Chem. Soc.* **2018**, *140*, 16438−16441.
(41) Li, X.; Gao, Q.; Wang, J.; Chen, Y.; Chen, Z.-H.; Xu, H.-S.; Tang, W.; Leng, K.; Ning, G.-H.; Wu, J.; Xu, Q.-H.; Quek, S. Y.; Lu, Y.; Loh, K. P. Tuneable near White-Emissive Two-Dimensional Covalent Organic Frameworks. *Nat. Commun.* **2018**, *9*, 2335.
(42) Li, L.; Lu, F.; Xue, R.; Ma, B.; Li, Q.; Wu, N.; Liu, H.; Yao, W.; Guo, H.; Yang, W. Ultrastable Triazine-Based Covalent Organic Framework with an Interlayer Hydrogen Bonding for Supercapacitor Applications. *ACS Appl. Mater. Interfaces* **2019**, *11*, 26355−26363.
(43) Alahakoon, S. B.; Tan, K.; Pandey, H.; Diwakara, S. D.; McCandless, G. T.; Grinffiel, D. I.; Durand-Silva, A.; Thonhauser, T.; Smaldone, R. A. 2D-Covalent Organic Frameworks with Interlayer Hydrogen Bonding Oriented through Designed Nonplanarity. *J. Am. Chem. Soc.* **2020**, *142*, 12987−12994.
(44) Zhu, D.; Alemany, L. B.; Guo, W.; Verduzco, R. Enhancement of Crystallinity of Imine-Linked Covalent Organic Frameworks via Aldehyde Modulators. *Polym. Chem.* **2020**, *11*, 4464−4468.
(45) Haase, F.; Lotsch, B. V. Solving the COF Trilemma: Towards Crystalline, Stable and Functional Covalent Organic Frameworks. *Chem. Soc. Rev.* **2020**, *49*, 8469−8500.
(46) Doonan, C.; Riccò, R.; Liang, K.; Bradshaw, D.; Falcaro, P. Metal−Organic Frameworks at the Biointerface: Synthetic Strategies and Applications. *Acc. Chem. Res.* **2017**, *50*, 1423−1432.
(47) Chae, H. K.; Siberio-Perez, D. Y.; Kim, J.; Go, Y.; Eddaoudi, M.; Matzger, A. J.; O'Keeffe, M.; Yaghi, O. M. A Route to High Surface Area, Porosity and Inclusion of Large Molecules in Crystals. *Nature* **2004**, *427*, 523−527.
(48) Herbert, F. C.; Abeyrathna, S. S.; Abeyrathna, N. S.; Wijesundara, Y. H.; Brohlin, O. R.; Carraro, F.; Amenitsch, H.; Falcaro, P.; Luzuriaga, M. A.; Durand-Silva, A.; Diwakara, S. D.; Smaldone, R. A.; Meloni, G.; Gassensmith, J. J. Stabilization of Supramolecular Membrane Protein−Lipid Bilayer Assemblies through Immobilization in a Crystalline Exoskeleton. *Nat. Commun.* **2021**, *12*, 2202.
(49) Oliveira, F. L.; de S. França, A.; de Castro, A. M.; Alves de Souza, R. O. M.; Esteves, P. M.; Gonçalves, R. S. B. Enzyme Immobilization in Covalent Organic Frameworks: Strategies and Applications in Biocatalysis. *ChemPlusChem* **2020**, *85*, 2051−2066.
(50) Sun, Q.; Fu, C.-W.; Aguila, B.; Perman, J.; Wang, S.; Huang, H.-Y.; Xiao, F.-S.; Ma, S. Pore Environment Control and Enhanced Performance of Enzymes Infiltrated in Covalent Organic Frameworks. *J. Am. Chem. Soc.* **2018**, *140*, 984−992.
(51) Li, H.; Ding, J.; Guan, X.; Chen, F.; Li, C.; Zhu, L.; Xue, M.; Yuan, D.; Valtchev, V.; Yan, Y.; Qiu, S.; Fang, Q. Three-Dimensional Large-Pore Covalent Organic Framework with Stp Topology. *J. Am. Chem. Soc.* **2020**, *142*, 13334−13338.
(52) Benyettou, F.; Kaddour, N.; Prakasam, T.; Das, G.; Sharma, S. K.; Thomas, S. A.; Bekhti-Sari, F.; Whelan, J.; Alkhalifah, M. A.; Khair, M.; Traboulsi, H.; Pasricha, R.; Jagannathan, R.; Mokhtari-Soulimane, N.; Gándara, F.; Trabolsi, A. In Vivo Oral Insulin Delivery via Covalent Organic Frameworks. *Chem. Sci.* **2021**, *12*, 6037−6047.
(53) Carlsson, N.; Gustafsson, H.; Thörn, C.; Olsson, L.; Holmberg, K.; Åkerman, B. Enzymes Immobilized in Mesoporous Silica: A Physical−Chemical Perspective. *Adv. Colloid Interface Sci.* **2014**, *205*, 339−360.
(54) Gößl, D.; Singer, H.; Chiu, H.-Y.; Schmidt, A.; Lichtnecker, M.; Engelke, H.; Bein, T. Highly Active Enzymes Immobilized in Large Pore Colloidal Mesoporous Silica Nanoparticles. *New J. Chem.* **2019**, *43*, 1671−1680.
(55) Liang, W.; Carraro, F.; Solomon, M. B.; Bell, S. G.; Amenitsch, H.; Sumby, C. J.; White, N. G.; Falcaro, P.; Doonan, C. J. Enzyme Encapsulation in a Porous Hydrogen-Bonded Organic Framework. *J. Am. Chem. Soc.* **2019**, *141*, 14298−14305.
(56) Bacakova, L.; Vandrovcova, M.; Kopova, I.; Jirka, I. Applications of Zeolites in Biotechnology and Medicine − a Review. *Biomater. Sci.* **2018**, *6*, 974−989.
(57) Fujita, D.; Suzuki, R.; Fujii, Y.; Yamada, M.; Nakama, T.; Matsugami, A.; Hayashi, F.; Weng, J.-K.; Yagi-Utsumi, M.; Fujita, M. Protein Stabilization and Refolding in a Gigantic Self-Assembled Cage. *Chem* **2021**, *7*, 2672−2683.
(58) Pédelacq, J.-D.; Cabantous, S.; Tran, T.; Terwilliger, T. C.; Waldo, G. S. Engineering and Characterization of a Superfolder Green Fluorescent Protein. *Nat. Biotechnol.* **2006**, *24*, 79−88.
(59) Luzuriaga, M. A.; Benjamin, C. E.; Gaertner, M. W.; Lee, H.; Herbert, F. C.; Mallick, S.; Gassensmith, J. J. ZIF-8 Degrades in cell media, serum, and some—but not all—common laboratory buffers. *Supramol. Chem.* **2019**, *31*, 485−490.
(60) Tutol, J. N.; Kam, H. C.; Dodani, S. C. Identification of mNeonGreen as a pH-Dependent, Turn-On Fluorescent Protein Sensor for Chloride. *ChemBioChem* **2019**, *20*, 1759−1765.
(61) Uribe-Romo, F. J.; Doonan, C. J.; Furukawa, H.; Oisaki, K.; Yaghi, O. M. Crystalline Covalent Organic Frameworks with Hydrazone Linkages. *J. Am. Chem. Soc.* **2011**, *133*, 11478−11481.

https://doi.org/10.1021/jacs.1c12020
J. Am. Chem. Soc. XXXX, XXX, XXX−XXX